


Field-Free Magnetization Switching by an Acoustic Wave

I.S. Camara,¹ J.-Y. Duquesne,¹ A. Lemaître,² C. Gourdon,¹ and L. Thevenard^{1,*}

¹*Sorbonne Université, CNRS, Institut des Nanosciences de Paris, 4 place Jussieu, 75252 Paris, France*

²*Centre de Nanosciences et de Nanotechnologies, CNRS, Université Paris-Sud, Université Paris-Saclay, 91460 Marcoussis, France*

 (Received 4 September 2018; revised manuscript received 9 November 2018; published 23 January 2019)

Surface acoustic waves (SAWs) propagating on magnetostrictive ferromagnets can induce magnetization reversal: their weak damping and mature technology make them ideal for remote wave control of magnetic bits. Experimental demonstrations of this spectacular coupling have so far required the simultaneous application of a static magnetic field. We show here SAW-driven all-acoustic switching (AAS) over millimetric distances. It relies on the triggering of magnetization precession of a uniaxial in-plane magnetized film by acoustic ferromagnetic resonance at zero field. Moreover, the absence of a biasing field enables toggling between the two equilibrium magnetic states for over 20 consecutive acoustic pulses. This proof-of-concept opens up an alternative path to magnetic-bit manipulation.

DOI: [10.1103/PhysRevApplied.11.014045](https://doi.org/10.1103/PhysRevApplied.11.014045)

I. INTRODUCTION

The switching of magnetic bits without the requirement for magnetic fields has been a constant quest in the spintronics and nanomagnetism communities, as it would enable a denser packing and easier addressing of magnetic bits in logic and memory devices, with limited cross talk. This search has been rewarded by the discovery of all-optical [1], electric-field, and current-induced magnetization switching [2–7]. For the latter two, however, the necessity for biasing fields remains ubiquitous, whether spin transfer, spin-orbit torques, or electric-field modulations of the anisotropy are in play. A recently developed alternative for magnetization switching is the use of acoustic waves [8–15]. The effective field generated by Rayleigh waves through inverse magnetostriction can switch magnetization efficiently in magnetostrictive thin films of both in-plane and out-of-plane anisotropies [14,15]. In these references, the mechanism was ascribed to resonant switching [8,9]: the SAW triggers a highly nonlinear large-amplitude magnetization rotation around a bias (resonance) field chosen to match the magnetic precession with the acoustic frequencies—typically 0.1–1 GHz. One way to eliminate the need for this field is to engineer a system in which the precession frequency matches the acoustic frequency at zero field. This is the key ingredient of our results: the thermal dependence of magnetic parameters in (Ga,Mn)As, a dilute magnetic semiconductor used as a demonstrator to achieve zero-magnetic-field surface-acoustic-wave (SAW) switching at a well-chosen temperature. Moreover, we demonstrate toggling between the two equilibrium

magnetic states by over 20 consecutive acoustic pulses, opening the way for field-free wave control of magnetization.

II. THE SAMPLE

The experiments are performed on a 45-nm-thick layer of (Ga_{0.95},Mn_{0.05})As grown by molecular-beam epitaxy on an unintentionally doped GaAs (001) substrate. The Curie temperature T_C reaches 120 K after a 16 h/200°C anneal. The layer has a strong in-plane uniaxial anisotropy along $[1\bar{1}0]$ up to T_C (a 1 mT coercive field at $T = 100$ K). For more details on this sample, see Ref. [15]. A 2×2 mm² magnetic mesa is defined by wet etching [Fig. 1(a)]. To excite and detect surface-acoustic Rayleigh waves, 60 nm-thick Al interdigitated transducers (IDTs) are deposited on either side of the mesa by lift-off. The “split-44” transducer design [16] is used: 15 pairs of four equipotential and equispaced digits that can be excited by a radio-frequency (rf) voltage. With a nominal base periodicity of $\lambda = 20$ μm, SAWs can be excited along the easy $[1\bar{1}0]$ axis at four frequencies nf_0 , with $n = 1, 3, 5,$ and 7 and $f_0 = V_r/\lambda = 141$ MHz, where V_r is the Rayleigh wave velocity. Here, we will only present work at $7f_0 = 990$ MHz, as it was shown to be the value that maximizes the switching efficiency [15].

III. ZERO-FIELD SAW-DRIVEN SWITCHING

To evaluate the effect of a single SAW burst on the layer magnetization, we perform longitudinal Kerr microscopy (632-nm LED illumination, NA = 0.4 objective). The sample magnetization is initialized as $+\mathbf{M}_0||[1\bar{1}0]$ with a permanent magnet and a reference image is acquired

*thevenard@insp.jussieu.fr

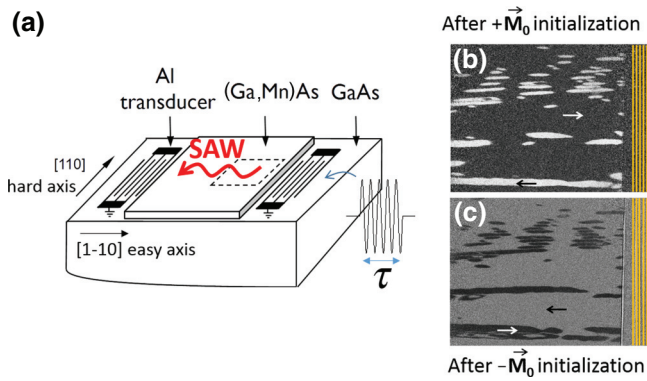


FIG. 1. (a) A schematic of the setup. For the switching experiments, Kerr microscopy images are taken over the area delimited by the dashed contour. For SAW FMR experiments (Fig. 3), τ -long pulses are applied to the right transducer. The field is applied along the hard axis [110] and the opposite transducer detects the acoustic echo. (b),(c) Kerr microscopy differential images ($306 \times 410 \mu\text{m}^2$) after a single 250 ns-long SAW burst at $T = 100$ K ($B = 0$ mT, $P_{\text{rf}} = 31$ dBm), and opposite initializations. The black and white arrows indicate the magnetization direction.

close to the emitting transducer [the dashed contour in Fig. 1(a)]. A single 250-ns-long rf pulse (990 MHz) is then applied to the IDT using a Keysight N5172B generator; an image is then taken and divided by the reference one in order to show the switched areas in normalized contrast. A field-regulated Caylar coil ensures that the external field is maintained at $B = 0 \pm 0.1$ mT at the sample location. Since we expect the resonance fields to decrease with increasing temperature, the temperature is set to $T = 100$ K, sufficiently close to the Curie temperature to expect low-field resonance with the SAW, as will be shown in Sec. IV, but far away enough to maintain a saturation magnetization of 20 kA m^{-1} .

Figure 1(b) shows that after the SAW pulse, the magnetization has switched in certain locations (the white domains). No field-free switching is observed at low rf power or when the transducer is excited out of its resonance bandwidth (e.g., at 980 MHz), ruling out an influence of heating or of the electromagnetic rf radiation from the IDTs. Elongated oblong domains are formed, a few tens of microns wide and up to $300 \mu\text{m}$ long. Similar shapes are observed after resonant switching under a field at 20 K [15]. This is explained as follows. At both of these temperatures, the SAW makes the magnetization oscillate between one equilibrium position and the other as soon as the absolute value of the strain reaches a certain threshold. When the rf excitation is stopped, the final magnetic configuration depends critically on the sign of the strain as it drops down to zero and once more crosses the threshold [8,9,14]. Micromagnetic simulations clearly show that a small dispersion of the sample magnetoelastic coefficients makes the SAW switching unequally efficient across the

layer, since the threshold depends on the detuning between the local precession frequency and the SAW frequency and on the strain amplitude [15]. This leads to the formation of extended patches of switched magnetization, in patterns that vary with the combination of P_{rf} and f_{SAW} that is used [as evidenced by comparing Figs. 1(b), 2(a), and 4]. Finally, note that the fairly long burst length used for switching is imposed by the long acoustic rise times of our device (90 ns), the IDT having been designed for narrow-bandwidth multiple-harmonic excitation, rather than short transients.

Initializing $-\mathbf{M}_0$ this time and applying the same SAW burst shows that switching also occurs [the black domains in Fig. 1(c)] and that some areas reverse regardless of the initial saturation: $-\mathbf{M}_0$ or $+\mathbf{M}_0$ [17]. This is in stark contrast to the resonant switching observed under a field at 20 K: minute variations of the field alignment with the hard axis across the sample prevent some areas from switching with the same efficiency from $-\mathbf{M}_0$ or $+\mathbf{M}_0$ initial configurations [15]. A similar favoring of one magnetization configuration over another was also routinely seen in the early days of current-driven precessional spin-valve switching [4], an influence of the polarizing-layer dipolar field. An efficient solution was the use of a synthetic antiferromagnet as polarizer to limit the influence of biasing fields on the free layer [18]. Here, suppression of the need for a field by working at higher temperature proves to be a fruitful strategy to balance the $-\mathbf{M}_0 \rightarrow +\mathbf{M}_0$ and $+\mathbf{M}_0 \rightarrow -\mathbf{M}_0$ switching probabilities.

Let us emphasize that the similarity between the switched patterns starting from $+\mathbf{M}_0$ or $-\mathbf{M}_0$ also rules out the possibility that switching is due to a spurious static field along the *easy* axis, where domain nucleation could be favored by the SAW: it would then only be efficient starting

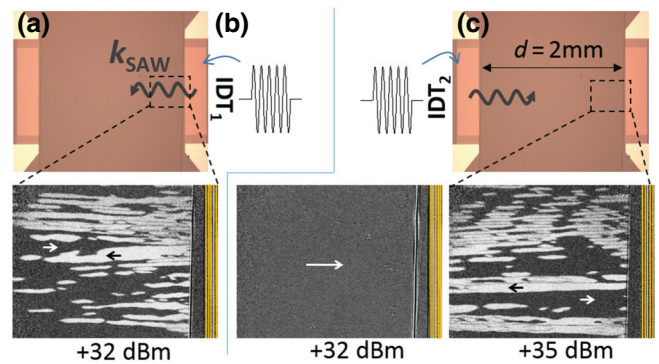


FIG. 2. Zero-field SAW-driven magnetization switching following a 250-ns-long 987-MHz rf pulse applied to the right (a) or left (b),(c) transducer (images $306 \times 410 \mu\text{m}^2$). When observing far from the excitation, the acoustic and magneto-acoustic losses need to be compensated to obtain a similar switching efficiency; hence the larger power (+35 dBm) needed for excitation through IDT₂.

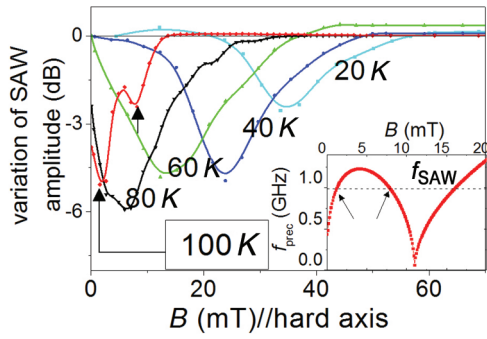


FIG. 3. The relative transmitted SAW amplitude versus the hard-axis field, at high rf power. Inset: the field dependence of the $T = 100$ K precession frequency, calculated taking into account the anisotropy constants determined by cavity FMR. In both graphs, the arrows point to the resonance conditions for which the precession frequency most closely matches $f_{\text{SAW}} = 990$ MHz.

from one configuration. Contrary to what we believe to be a *resonant* switching route here, this would be a *nonresonant* SAW-assisted mechanism, which has already been evidenced in (Ga,Mn)(As,P), Co/Pt, and FeGa [10,11,13].

To evaluate the distance from the exciting transducer up to which this effect remains efficient, we take two magneto-optical images close to the right transducer IDT₁, after applying an rf pulse either to IDT₁ [Fig. 2(a)] or to the opposite one, IDT₂, 2 mm away [Figs. 2(b) and 2(c)]. Switching remains efficient provided that the applied power is increased by +3 dB in the latter case. This compensates for the SAW magneto-acoustic attenuation (see further the $T = 100$ K SAW FMR curve in Fig. 3), to a lesser degree for the native attenuation of the SAW in GaAs [19] and for the weak asymmetry of the IDT transduction efficiencies. A similar long-distance efficiency has been shown when using the SAW to reduce transiently domain nucleation barriers [13]. This once more demonstrates the relevance of SAWs for remote switching.

IV. ZERO-FIELD SAW-DRIVEN FERROMAGNETIC RESONANCE

To assess whether resonant SAW-induced magnetization precession is indeed the mechanism responsible for this zero-field SAW-driven reversal, we now present SAW-driven ferromagnetic resonance experiments (SAW FMR). Obtaining this resonance is a prerequisite for magnetization switching [14,15]. Here, the layer is magnetically initialized $+\mathbf{M}_0$ along the easy axis $[1\bar{1}0]$ and 400 ns-long rf bursts at a 1 kHz repetition rate are delivered to IDT₁. The transmitted SAW amplitude and phase variations are measured on the echo detected at IDT₂ as the in-plane field is increased [Fig. 1(a)]. With the applied field along the hard axis, the magnetization is progressively oriented away from the easy axis, leading to a decrease of the magnetization precession frequency (inset

of Fig. 3). The magnetization is mainly coupled to the SAW longitudinal strain via the anisotropic magnetoelastic coupling coefficient, commonly called B_2 in metallic ferromagnets [20]. The transverse strain intervenes to a lesser degree, via weaker higher-order magnetoelastic coupling coefficients [15].

Figure 3 shows the SAW amplitude variations for $T = 20$ –100 K, at $f_{\text{SAW}} = 990$ MHz at high SAW power ($P_{\text{rf}} \approx 35$ dBm). At all temperatures, a resonant absorption occurs at the field for which the mean precession frequency most closely matches f_{SAW} [15,21,22], a clear signature of SAW-induced magnetization precession. The resonant field decreases from 35 mT at 20 K to about 1.5 mT at 100 K. At this temperature, a second resonance peak is present at a higher field, 8 mT, where the precession frequency crosses f_{SAW} a second time (inset of Fig. 3).

Let us now discuss the choice of temperature and rf power for the field-free switching experiments. At sufficiently low SAW power (not shown), the transmitted SAW amplitude varies linearly with the incoming one and the precession amplitude is small, as evidenced experimentally, and is proportional to the strain amplitude [23]. At zero field, there is no absorption and no torque on the magnetization either [21,22]. At the typical powers and temperature used here (+31–35 dBm, $T = 100$ K), however, the SAW transmission becomes nonlinear and the resonance shifts down to lower field, with the SAW FMR absorption remaining finite at zero field (Fig. 3). The SAW-induced magnetization dynamics are expected to become highly nonlinear with complex trajectories [9], a prerequisite for precessional switching [9,14]. A certain level of absorption must, however, be reached to observe field-free switching: none is seen at 80 K (at the maximum available rf power) where there is a weaker zero-field SAW attenuation than at 100 K.

V. ZERO-FIELD SAW-DRIVEN MAGNETIZATION TOGGLING

In the macrospin vision of precessional switching, the final magnetic configuration depends on the compressive or tensile nature of the strain as it decays down to zero at the end of the burst and crosses the switching threshold [8,9,14]. For consecutive identical rf bursts, it should thus be possible to toggle the magnetization between $-\mathbf{M}_0$ and $+\mathbf{M}_0$ with high fidelity, a determinism that is critical when manipulating magnetically encoded information. At $T = 20$ K, such reversibility cannot be obtained: the application of successive pulses barely modifies the switched magnetization pattern, because even minute misalignments of the bias field with the static local magnetization robustly favor one configuration over the other [15].

In order to test whether magnetization can be switched locally and repeatedly between $\pm\mathbf{M}_0$ by an acoustic wave, *without field* this time we proceed as follows. At $T = 100$

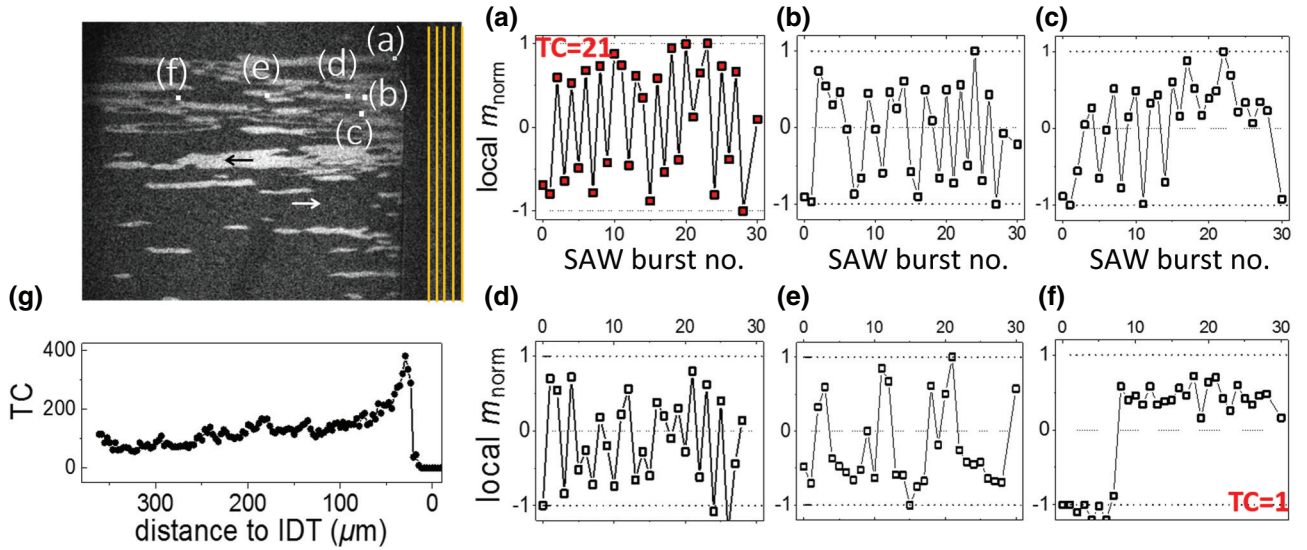


FIG. 4. (a)–(f) Zero-field toggling behavior under successive 250 ns-long 990 MHz SAW bursts at $T = 100$ K ($B = 0$ mT, $P_{\text{rf}} = 35$ dBm, image $306 \times 410 \mu\text{m}^2$), starting from a $+\mathbf{M}_0$ configuration: normalized local magnetization of selected $10 \times 10 \text{ pixel}^2$ bins. The labels on the image locate the position of each bin with respect to the IDT. (g) The toggling count (TC, defined in the Supplemental Material) summed over the SAW wavefront, as a function of the distance to the SAW emitter.

K, a reference image is taken after a $+\mathbf{M}_0$ initialization and 30 consecutive rf bursts of nominally identical phase and duration are applied at 10-s intervals, with a Kerr image being taken after each one. At the end of the series, another reference image is taken after saturating $-\mathbf{M}_0$. A spatial analysis of the local intensity $I(\mathbf{r})$ of these images is performed numerically to obtain the local normalized magnetization of the n th burst image: $m_{\text{norm}}^n(\mathbf{r}) = 2((I^n(\mathbf{r}) - I_{+\mathbf{M}_0}(\mathbf{r})) / (I_{-\mathbf{M}_0}(\mathbf{r}) - I_{+\mathbf{M}_0}(\mathbf{r}))) - 1$. This value between -1 and $+1$ corresponds to the average normalized magnetization of a $2.9 \times 2.9 \mu\text{m}^2$ area ($10 \times 10 \text{ pixel}^2$ bin) centered around \mathbf{r} . Figures 4(a)–4(f) show the switching behavior for a few representative bins. Bin (a) is located about $36 \mu\text{m}$ from the exciting IDT and excellent toggling is observed between the $-\mathbf{M}_0$ and $+\mathbf{M}_0$ states. As the distance to the exciting transducer increases [bins (b) and (c) at approximately $70 \mu\text{m}$, (d) at approximately $80 \mu\text{m}$, and (e) at $170 \mu\text{m}$], this behavior becomes less robust overall. Bin (f) shows only one switching event in the 30-SAW-pulses series and does not switch back to its initial state unless the sample is resaturated. Instead, consecutive SAW bursts result in slow domain expansion, a compelling phenomenon that will be developed in an upcoming communication. A similar phenomenology is observed when starting from the $-\mathbf{M}_0$ uniform configuration.

We define the toggling count, TC, as the number of large-contrast jumps in the 30-burst series (for details, see the Supplemental Material). While some pockets of high TCs can be found both close to the transducer and far away from it (see the Supplemental Material [17]), vertical averaging of the toggling efficiency shows a clear overall

degradation when moving away from the IDT [Fig. 4(g)]. To explain this in the framework of precessional switching, the acoustic field seen at a given location should be significantly modified from burst to burst, for instance, by spatial and temporal phase fluctuations of the SAW wavefront, which would induce decoherence in the resonant switching process. Variations of the Rayleigh wave velocity (due to a temperature drift or modification of the sample surface with time) can be safely discarded as a likely explanation, since they would only delay the arrival of the SAW burst but not influence its end phase, i.e., the strain sign as it crosses the switching threshold. Instead, an incoherent scattering of the wave as it travels on the multi-magnetic-domain layer can be invoked. The numerous magnetic domain walls that it must cross may modify its phase and amplitude, acting as a scattering landscape that varies after each burst. Finally, competing mechanisms might also contribute to stochastic nonresonant reversals, such as the aforementioned transient decrease of domain-nucleation barriers or domain-wall motion and/or creation.

VI. CONCLUSIONS

We present a proof-of-concept demonstration of SAW-driven all-acoustic switching. Working on the dilute magnetic semiconductor (Ga,Mn)As, we rely on the steep decrease of the resonance field matching precession and SAW frequency with increasing temperature to reverse magnetization over millimetric distances. Deterministic two-way toggling is evidenced in several spots but the overall efficiency is shown to decrease with the distance to

the transducer, a possible consequence of the multidomain configuration due to the dispersion of the magnetic parameters and the large sample size. The optimal configuration for zero-field SAW switching should therefore rely on a room-temperature ferro- or ferrimagnet exhibiting a combination of a low precession frequency and yet high magnetostriction, structured into monodomain structures, and SAWs excited by an impedance-matched IDT centered around a few GHz. Complemented by wave-front shaping or the focusing IDTs, this will enable the spatial selection of a magnetic structure using acoustics.

ACKNOWLEDGMENTS

This work has been partly supported by the French Agence Nationale de la Recherche (ANR13-JS04-0001-01) and the French RENATECH network. We acknowledge M. Bernard (Institut des Nanosciences de Paris) for technical assistance.

-
- [1] S. Mangin, M. Gottwald, C.-H. Lambert, D. Steil, V. Uhler, L. Pang, M. Hehn, S. Alebrand, M. Cinchetti, G. Malinowski, Y. Fainman, M. Aeschlimann, and E. E. Fullerton, Engineered materials for all-optical helicity-dependent magnetic switching, *Nat. Mater.* **13**, 286 (2014).
- [2] W. K. Hiebert, L. Lagae, and J. De Boeck, Spatially inhomogeneous ultrafast precessional magnetization reversal, *Phys. Rev. B* **68**, 020402 (2003).
- [3] I. N. Krivorotov, Time-domain measurements of nanomagnet dynamics driven by spin-transfer torques, *Science* **307**, 228 (2005).
- [4] C. Papusoi, B. Delaët, B. Rodmacq, D. Houssameddine, J.-P. Michel, U. Ebels, R. C. Sousa, L. D. Buda-Prejbeanu, and B. Dieny, 100 ps precessional spin-transfer switching of a planar magnetic random access memory cell with perpendicular spin polarizer, *Appl. Phys. Rev.* **95**, 072506 (2009).
- [5] D. Bedau, H. Liu, J.-J. Bouzaglou, A. D. Kent, J. Z. Sun, J. A. Katine, E. E. Fullerton, and S. Mangin, Ultrafast spin-transfer switching in spin valve nanopillars with perpendicular anisotropy, *Appl. Phys. Rev.* **96**, 022514 (2010).
- [6] Y. Shiota, T. Nozaki, F. Bonell, S. Murakami, T. Shinjo, and Y. Suzuki, Induction of coherent magnetization switching in a few atomic layers of FeCo using voltage pulses, *Nat. Mater.* **11**, 39 (2011).
- [7] H. Zhang, Z. Hou, J. Zhang, Z. Zhang, and Y. Liu, Precession frequency and fast switching dependence on the in-plane and out-of-plane dual spin-torque polarizers, *Appl. Phys. Rev.* **100**, 142409 (2012).
- [8] O. Kovalenko, T. Pezeril, and V. V. Temnov, New Concept for Magnetization Switching by Ultrafast Acoustic Pulses, *Phys. Rev. Lett.* **110**, 266602 (2013).
- [9] L. Thevenard, J.-Y. Duquesne, E. Peronne, H. J. von Bardeleben, H. Jaffrès, S. Ruttala, J.-M. George, A. Lemaître, and C. Gourdon, Irreversible magnetization switching using surface acoustic waves, *Phys. Rev. B* **87**, 144402 (2013).
- [10] W. Li, B. Buford, A. Jander, and P. Dhagat, Acoustically assisted magnetic recording: A new paradigm in magnetic data storage, *IEEE Trans. Mag.* **50**, 3100704 (2014).
- [11] U. Singh and S. Adenwalla, Spatial mapping of focused surface acoustic waves in the investigation of high frequency strain induced changes, *Nanotechnology* **26**, 255707 (2015).
- [12] S. Davis, J. A. Borchers, B. B. Maranville, and S. Adenwalla, Fast strain wave induced magnetization changes in long cobalt bars: Domain motion versus coherent rotation, *J. Appl. Phys.* **117**, 063904 (2015).
- [13] L. Thevenard, I. S. Camara, J.-Y. Prieur, P. Rovillain, A. Lemaître, C. Gourdon, and J.-Y. Duquesne, Strong reduction of the coercivity by a surface acoustic wave in an out-of-plane magnetized epilayer, *Phys. Rev. B* **93**, 140405 (2016).
- [14] L. Thevenard, I. S. Camara, S. Majrab, M. Bernard, P. Rovillain, A. Lemaître, C. Gourdon, and J.-Y. Duquesne, Precessional magnetization switching by a surface acoustic wave, *Phys. Rev. B* **93**, 134430 (2016).
- [15] P. Kuszewski, I. S. Camara, N. Biarrotte, L. Becerra, J. von Bardeleben, W. Savero Torres, A. Lemaître, C. Gourdon, J.-Y. Duquesne, and L. Thevenard, Resonant magnetoacoustic switching: Influence of Rayleigh wave frequency and wavevector, *J. Phys.: Cond. Mat.* **30**, 244003 (2018).
- [16] F. J. R. Schülein, E. Zallo, P. Atkinson, O. G. Schmidt, R. Trotta, A. Rastelli, A. Wixforth, and H. J. Krenner, Fourier synthesis of radiofrequency nanomechanical pulses with different shapes, *Nat. Nanotechnol.* **10**, 512 (2015).
- [17] See the Supplemental Material at <http://link.aps.org/supplemental/10.1103/PhysRevApplied.11.014045> for details on the effect of the initial saturation and for the definition of the toggling count.
- [18] A. Vayssset, C. Papusoi, L. D. Buda-Prejbeanu, S. Bandiera, M. Marins de Castro, Y. Dahmane, J.-C. Toussaint, U. Ebels, S. Auffret, R. Sousa, L. Vila, and B. Dieny, Improved coherence of ultrafast spin-transfer-driven precessional switching with synthetic antiferromagnet perpendicular polarizer, *Appl. Phys. Rev.* **98**, 242511 (2011).
- [19] A. J. Slobodnik, GaAs acoustic-surface-wave propagation losses at 1 GHz, *Elec. Lett.* **8**, 307 (1972).
- [20] A. Hubert and R. Schäfer, *Magnetic Domains* (Springer, Berlin, 2000).
- [21] L. Dreher, M. Weiler, M. Pernpeintner, H. Huebl, R. Gross, M. Brandt, and S. Goennenwein, Surface acoustic wave driven ferromagnetic resonance in nickel thin films: Theory and experiment, *Phys. Rev. B* **86**, 134415 (2012).
- [22] L. Thevenard, C. Gourdon, J.-Y. Prieur, H. J. von Bardeleben, S. Vincent, L. Becerra, L. Largeau, and J.-Y. Duquesne, Surface-acoustic-wave-driven ferromagnetic resonance in (Ga,Mn)(As,P) epilayers, *Phys. Rev. B* **90**, 094401 (2014).
- [23] P. Kuszewski, J.-Y. Duquesne, L. Becerra, A. Lemaître, S. Vincent, S. Majrab, F. Margailan, C. Gourdon, and L. Thevenard, Optical Probing of Rayleigh Wave Driven Magneto-Acoustic Resonance, *Phys. Rev. Applied* **10**, 1 (2018).